POLITECNICO
MILANO 1863

SCUOLA DI INGEGNERIA INDUSTRIALE
E DELL'INFORMAZIONE

Executive Summary of the Thesis

Experimental and Computational Study of High-energy Radiotherapy Effects on Cardiac Implantable Electronic Devices with CR39 and MCNP

Laurea Magistrale in Nuclear Engineering - Ingegneria Nucleare

Author: Antonella Mele

Advisor: Prof. Marco Caresana

Co-advisor: Matteo Bolzonella

Academic year: 2020-2021

1. Introduction

Cardiac Implantable Electronic Devices (CIEDs) have proven to be an excellent tool for the treatment of patients suffering from heart diseases (e.g. arrhythmia) especially as a consequence of technological advances in the last decade. According to a study reported in literature, it is estimated that around 500,000 pacemakers (PM) and 100,000 implantable cardioverter-defibrillator (ICD) are implanted in Europe each year [1]. However, it is quite common, due to shared risk factors between the two pathologies, that the same patients are also diagnosed with a tumor during their life and that they must therefore undergo radiotherapy treatments. Hence, there is the need to develop guidelines that allow the correct management of these patients, as it is widely recognized that malfunctions in the devices may be induced directly by exposure to ionizing radiation and indirectly by secondary particles produced in the treatment room by the interaction of high-energy photons ($>$ 10 MV) with the LINAC's head structure and the maze walls [2, 3]. The present work aims at characterizing the secondary photoneutron field, that contaminates the X-ray beam during high-energy treatments, inside a phantom simulating the patient's bust. Specifically, we want to investigate the thermal neutron fluence in the region where a CIED is implanted and compare this value with that for which a considerable incidence of malfunctions has been experimentally reported following irradiation with thermal neutrons ($\sim 10^9 \frac{\mathrm{n}}{\mathrm{cm}^2}$) [4]. To experimentally assess the quantity of interest, CR39 solid state nuclear track detectors (SSNTDs) coupled to boron carbide converters enriched in B-10 were used. The experimental campaign took place in three different hospitals: *Ospedale di Circolo e Fondazione Macchi - Azienda Socio Sanitaria Territoriale (ASST) dei Sette Laghi* hospital in Varese housing a *DHX Clinac* by *Varian Medical Systems*, *San Luca - Azienda Usl Toscana nord ovest* hospital in Lucca housing a *Synergy 3028* medical LINAC by *Elekta* and *Ospedale Maggiore - Azienda Sanitaria Universitaria Giuliano Isontina (ASUGI)* hospital in Trieste housing a *Elekta Synergy 3028* linear accelerator.

In addition, a computational model of the Elekta Synergy LINAC head and the treat-

ment room of the Azienda Sanitaria Universitaria Giuliano Isontina (ASUGI) in Trieste was improved with the addition of a phantom, designed to reproduce the one used in the experiments and aimed at simulating the patient's body, and validated by means of experimental data. This model is based on the Monte Carlo MCNP 6.2 code.

2. Materials & Methods

2.1. The detection system

The thermal neutron fluence was estimated using a detector made up of a CR39 SSNTD of dimensions 15x15x1.5 mm^3 in combination with 99% B-10 enriched boron carbide film acting as a converter, via the $^{10}B(n,\alpha)^{7}Li$ reaction. Neutrons are absorbed by the boron nuclei and in their place secondary charged particles are emitted which release their energy within the sensitive volume of the CR39. Along the path followed by the ion, the material presents damage at the molecular bonds level that give rise to what is called *latent track*. A chemical treatment, known as *etching*, will be required to enlarge the track to the point they can be observed using an optical system. In particular, this is made possible by the different erosion speed of the material, which is higher along the latent track than the *bulk*, that is, the undamaged material.

CR39 were provided by two different manufacturers, Track Analysis System Ltd (TASL) and Reinforced ThermoPlastics Company (RTP), and their sensitivity to thermal neutrons was evaluated by exposing 12 TASL and 25 RTP detectors to a nominal thermal neutron flux (φ_{th}) of 492 $cm^{-2}s^{-1}$ emitted by the ESTHER (Expanded Source-based THERmal neutron field) facility at Politecnico di Milano, hosting a moderated AmBe source. To isolate the thermal component of the spectrum 3 RTP and 5 TASL CR39 were shielded through cadmium plates.

After the exposure, CR39 were etched with a bath in an aqueous solution 6.25 mol/L of sodium hydroxide (NaOH) at 97.3 ± 0.1 °C for 40 minutes. Then, they were analyzed using the Politrack® system, consisting in an optical microscope used for scanning SSNTDs and performing a morphological analysis of the tracks. Table 1 summarizes the measured calibration factors $f_{c,th}$ $[\frac{n}{trk}]$ to convert track density into neutron fluence.

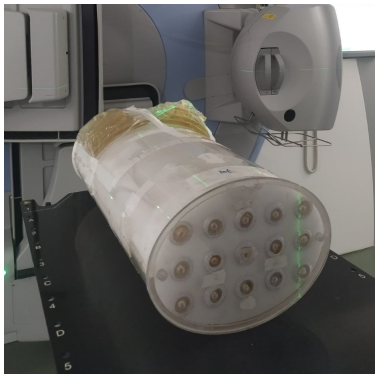

Figure 1: BOMAB-like phantom trunk developed by University of Pisa.

Detectors producer	$f_{c,th}$ $[\frac{n}{trk}]$	Relative Uncertainty (1σ)
RTP	142.57	3%
TASL	129.52	3%

Table 1: CR39 calibration factors.

2.2. BOMAB-like phantom

During the experiments a BOMAB-like phantom designed and developed at the University of Pisa was used to accurately reproduce the conditions of real therapy sessions. It is an elliptic cylinder made with polymethyl methacrylate (PMMA) walls and with 15 through pipes in which it is possible to insert dosimeters or otherwise filled with PMMA spacers. It is 60 cm long, while the major and minor axis of the ellipse measure 29 cm and 21 cm, respectively. Therefore, it is suitable for simulating the trunk of a patient. Originally, it was filled with water, then substituted with paraffin. Moreover, it is possible to add two pyramidal structures made of a tissue-equivalent material above the phantom to mimic the breast (fig. 1).

2.3. Monte Carlo simulations

The computational Monte Carlo (MC) model, developed by the University of Trieste, included a detailed description of the *Elekta Synergy* accelerator head and the maze built in the treatment room at ASUGI (fig. 3). Their entire geometry was drawn using the computer-aided design software *AutoCad*. Then, the compatible

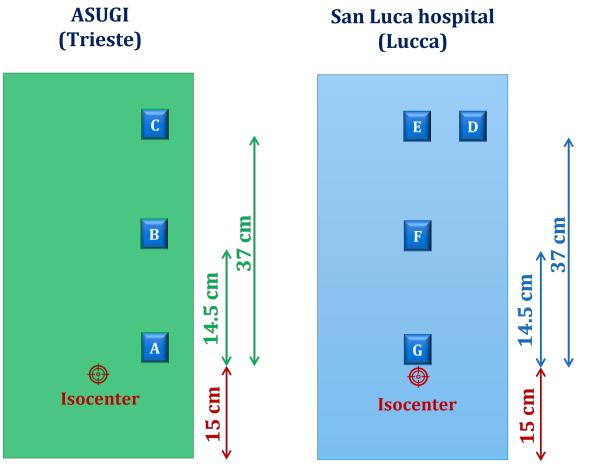

Figure 2: Detectors set-up used during the experimental measurements for the validation of the computational code at ASUGI and San Luca hospitals. This configuration is the one simulated in MCNP.

tool *MCNP Visual Editor* (MCNPXVised, version 22S) allowed to convert it into the format of an MCNP input file. To this computational setup, we added the model of the BOMAB-like phantom used during the experiments was also implemented with the purpose of simulating the presence of a patient. It is an elliptic cylinder, with the same size of the original one, made of water. Inside it we inserted cylindrical volumes, having the same radius as the phantom's channels (1 cm) and a height of 3 cm, centered about the points where, during the experiments, detectors were located (fig. 2) which were used to tally the (thermal) neutron fluence and to determine the photoneutron spectra therein. Moreover, a sphere with a volume of 1 cm^3 centered about the LINAC isocenter was included. In particular, the last volume was added to compute the photon dose at the isocenter.

Several variance reduction techniques (VRTs) were also implemented to optimize the computational code: energy cut-offs, cell importance and bremsstrahlung biasing. It should be noted that in the simulations the differences between the bunkers of the two hospitals in which the experiments, aimed at validating the code itself, were carried out are assumed to be negligible as the two have a similar structure.

3. Results

This section contains the results of the experimental measurements carried out at three different hospitals in Italy during which realistic therapy plans were simulated on the BOMAB phantom previously described. Uncertainties were computed as the sample standard deviation of the measurement combined with the uncertainty on the calibration factor. The relative uncertainty reported in the table corresponds to one standard deviation, 1σ.

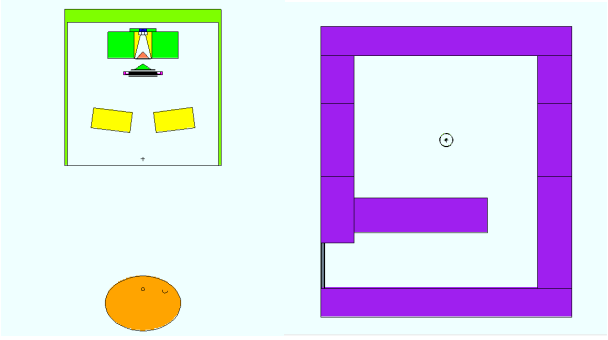

(a) (b)

Figure 3: 2D visualization of the (a) LINAC head and the phantom geometry simulated (Frontal view) and (b) the ASUGI treatment room geometry implemented in MCNP, xy plane.

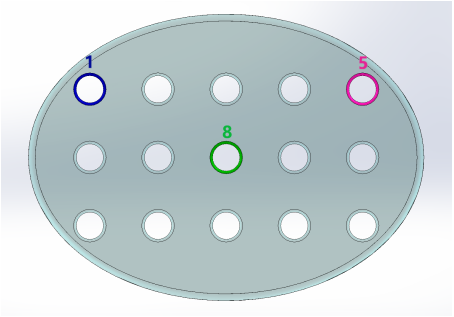

Figure 4: 2D rendering of a cross-sectional view of the BOMAB-like phantom developed by University of Pisa. Channel no.1 (in blue), no.5 (in fuchsia) and no.8 (in green) are highlighted since the devices were placed inside them during the experimental sessions.

3.1. Experimental measurements

Ospedale di Circolo e Fondazione Macchi (Varese)

The hospital houses a *DHX Clinac* by *Varian Medical Systems* which was used in photon mode, with a field size of 10x10 cm^2 to deliver a 18 MV treatment to the tumour area, i.e. a vertebra, repeated several times varying the moni-

tor units (MU) [1]. Detectors were inserted inside the channel no. 1 (fig. 4), 16 cm from the upper base of the phantom. In particular, to improve the statistics, two CR-39 with a boron converter between them were used for each irradiation

Results are reported in table 2: they show the thermal neutron fluence ($\Phi_{n,th}$) per MU delivered during the treatment.

Energy [MV]	MU delivered at isocenter	$\frac{\Phi_{n,th}}{MU}$ $[\frac{1}{cm^2 \cdot MU}]$	Relative uncertainty
18	20	1.75×10^5	4%
	40	1.63×10^5	5%
	100	9.03×10^4	3%

Table 2: Results obtained in Varese for the vertebra treatment at CIED site in terms of thermal neutron fluence per MU.

It should be noted that during those experiments it was not possible to use the Cd plates to exclude the contribute associated to the epithermal component of the neutron spectrum from the total one, because they were not available. However, the results obtained are still meaningful because *a)* the boron absorption cross section is considerably reduced in the range of epithermal energies (it decreases following the *1/v* law) making, *de facto*, the device less sensitive to epithermal neutrons and *b)* the thermal component of the neutron spectrum inside the water phantom prevails over the epithermal one, as also confirmed by MCNP simulations.

The order of magnitude of the estimated fluence is almost the same ($\sim 10^5 \frac{n}{cm^2 MU}$), except for the last one, which is slightly lower. This is due to CR39 saturation that occurs at very high track density levels (> 60.000 tr/cm^2), where the built-in correction algorithm of the reader for track overlapping corrections becomes less effective.

Azienda Sanitaria Universitaria Giuliano Isontina (ASUGI, Trieste)

The simulated treatment plan, based on real TAC images, was a 15 MV treatment delivered by the *Elekta Synergy 3028*, housed in the ASUGI hospital, to the iliac wing. It was repeated twice, in one case with bare detectors and in the other shielding them with cadmium.

[1]Note that for the purposes of this work it has been assumed that 100 MU = 1 Gy.

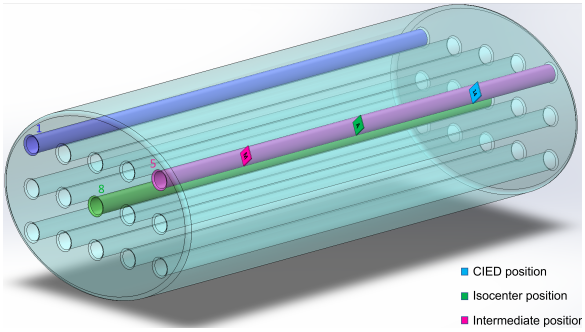

Figure 5: Detectors setup used during the experiments at ASUGI.

In these experiments a single CR39 per measurement was used, coupled with the boron film.

The purpose of these experiments was to study the thermal neutron fluence at the CIED site when the LINAC isocenter is located in a distal region with respect to the one where a cardiac device is implanted. Moreover, we wanted to investigate the fluence distribution along the phantom axis. Therefore, detectors were placed inside the channel no. 1, according to the configuration illustrated in fig. 5 for the case of the channel no. 5.

From data reported in table 3 we can conclude that the distribution of the thermal neutron fluence along the phantom's channel is quite constant and an increase of a factor 2 is observed when approaching the isocenter. Moreover, in the CIED position it is possible to notice a reduction of approximately a factor 5 in the thermal neutron fluence for the treatment plan carried out in Varese. However, it is useful to underline that the LINAC in Varese operated at 18 MV photon beam energy, while in Trieste at 15 MV.

Energy [MV]	Measuring position	$\frac{\Phi_{n,th}}{MU}$ $[\frac{1}{cm^2 \cdot MU}]$	Relative uncertainty
15	Channel no. 5, *intermediate* position	2.85×10^4	3%
	Channel no. 5 *isocenter* position	7.94×10^4	3%
	Channel no. 5, *CIED* position	$\mathbf{6.24\times10^4}$	**3%**

Table 3: Results obtained in Trieste for the iliac wing treatment in terms of thermal neutron fluence per MU. The highlighted row contains data that can be compared to the corresponding one in table 4.

San Luca Hospital (Lucca)

The San Luca Hospital hosts an *Elekta Synergy 3028* linear accelerator, like ASUGI. Therefore, in the first place, the same experiments conducted at ASUGI were repeated to verify if accelerators of the same manufacturer and model (placed in similar treatment rooms) produced the same thermal neutron fluence. So, one detector was placed in channel no. 1 at the CIED position to perform a direct comparison to the results obtained in Trieste, while the remaining three were disposed in channel no. 8 according to the set-up illustrated in fig. 5 for channel 5 to evaluate the fluence distribution.

After that, 10 and 15 MV breast treatments were simulated on the BOMAB-like phantom above which two breasts made of tissue equivalent material were placed. The devices were placed in channels no. 1 (directly underneath the irradiated breast) and no. 5 (below the contralateral breast with respect to the treated one) a few centimeters deep from the upper base of the phantom, in the CIED position.

Results are reported in table 4 and table 5. It was verified that the same treatment delivered using accelerators of the same manufacturer and model generates a completely comparable neutron fluence. Besides, the fluence distribution estimated by placing detectors in different points inside the phantom showed the same trend of the one observed at ASUGI, namely almost constant except near the isocenter.

Finally, data related to the breast treatment, once again, confirmed what has been said so far: along a channel, the CIED is exposed to a thermal neutron fluence of the order of $\sim 10^5$ $n \cdot cm^{-2} \cdot MU^{-1}$ and it is always a little bit higher at the isocenter.

Energy [MV]	Measuring position	$\frac{\Phi_{n,th}}{MU}$ $[\frac{1}{cm^2 \cdot MU}]$	Relative uncertainty
15	**Channel no. 5, *CIED* position**	**6.81×10^4**	**9%**
	Channel no. 8, *CIED* position	3.28×10^4	3%
	Channel no. 8, *intermediate* position	3.70×10^4	3%
	Channel no. 8, *isocenter* position	4.98×10^4	3%

Table 4: Results obtained in Lucca for the iliac wing treatment. The highlighted row contains data that can be compared to their corresponding one in table 3.

Energy [MV]	Measuring position	$\frac{\Phi_{n,th}}{MU}$ $[\frac{1}{cm^2 \cdot MU}]$	Relative uncertainty
10	Channel no. 1, CIED position	1.09×10^4	3%
	Channel no. 5, CIED position	7.38×10^3	5%
15	Channel no. 1, CIED position	3.62×10^4	4%
	Channel no. 5, CIED position	2.39×10^4	7%

Table 5: Results obtained in Lucca for the breast treatment.

3.2. Monte Carlo model validation

The computational model described in section 2.3 was validated comparing the experimental and simulated ratios between the thermal neutron fluence ($\Phi_{n,th}$) and the absorbed photon dose at the isocenter ($dose_{ph}$). These quantities were, respectively, measured and computed for a benchmark treatment delivered by the Elekta LINACs in Trieste and Lucca. The field size was set to 30x30 cm^2 and the isocenter positioned 15 cm from the bottom of the phantom and 4.5 cm deep from the surface. The detectors set-up is, instead, illustrated in fig. 2. The photon dose at the isocenter, instead, was calculated with the Treatment Planning System *Oncentra*.

The results are reported in table 6 and table 7. The MC code generally overestimates the calculated ratios: for example, we can observe that between the ratios referring to measurement positions A and B there is a difference of a factor 3. However, for the remaining points considered, the agreement is quite good and in any case the order of magnitude is the same. Moreover, it predicts the expected decreasing trend of the quantities under investigation when we move away from the isocenter. The relative uncertainty corresponding to 1σ is about 3% for 9×10^8 primary electrons simulated.

MCNP vs ASUGI (Trieste)

Measuring position	$\frac{\Phi^{exp}_{n,th}}{dose^{exp}_{ph}}$ $[\frac{n}{cm^2 \cdot Gy}]$	$\frac{\Phi^{MCNP}_{n,th}}{dose^{MCNP}_{ph}}$ $[\frac{n}{cm^2 \cdot Gy}]$	Error % $[\frac{data_{MCNP} - data_{exp}}{data_{MCNP}}]$
A	3.84×10^6	9.98×10^6	62%
B	1.27×10^6	5.05×10^6	75%
C	1.60×10^6	1.97×10^6	19%

Table 6: Comparison between the results obtained by Monte Carlo simulations and through experimental measures at ASUGI. The measuring positions refer to detectors code in fig. 2.

MCNP vs San Luca Hospital (Lucca)

Measuring position	$\frac{\Phi^{exp}_{n,th}}{dose^{exp}_{ph}}\left[\frac{n}{cm^2 \cdot Gy}\right]$	$\frac{\Phi^{MCNP}_{n,th}}{dose^{MCNP}_{ph}}\left[\frac{n}{cm^2 \cdot Gy}\right]$	Error % $\left[\frac{data_{MCNP}-data_{exp}}{data_{MCNP}}\right]$
G	6.35×10^6	8.29×10^6	23%
F	5.03×10^6	5.97×10^6	16%
E	2.26×10^6	3.03×10^6	32%
D	1.07×10^6	9.37×10^5	-14%

Table 7: Comparison between the results obtained by Monte Carlo simulations and through experimental measures at San Luca Hospital. The measuring positions refer to detectors code in fig. 2.

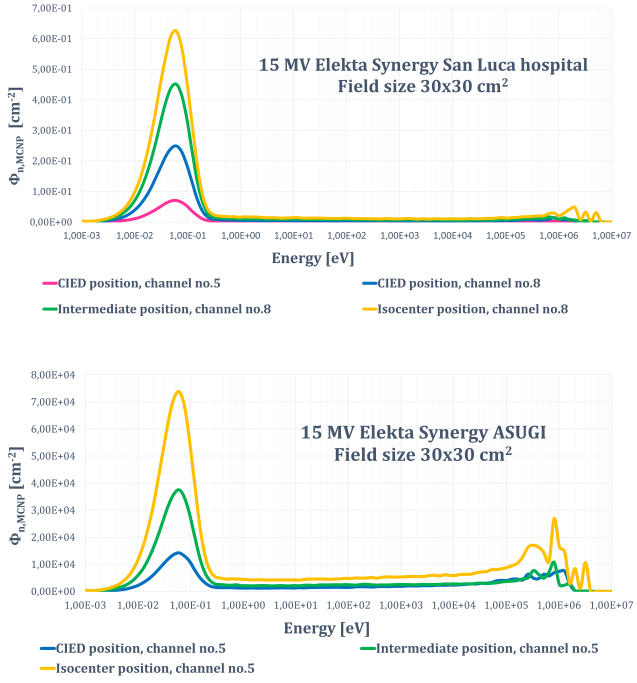

Figure 6: Photoneutrons spectra simulated using MCNP at different positions along the phantom axis.

A further confirmation of the capability of the code to reproduce the physics of the problem is given by the *photoneutron spectra* calculated at different positions inside the phantom (fig. 6), whose trend is comparable to those reported in literature [5].

At this point, since the code has been validated for the production and transport of electrons-photons-neutrons, it can be used in further studies, for example to perform an analysis of the risks that the patient faces during a more realistic session of radiotherapy as well as for the estimation of further quantities of interest in addition to those mentioned in this work.

4. Conclusions

The purpose of this study was to measure the photoneutron fluence produced during high-energy radiotherapy treatments by the interaction of the X-rays produced by LINACs and the high-Z materials of its head, as well as the bunker walls or the patient body itself. Specifically, we wanted to investigate the area next to the heart, where a cardiac implantable electronic device is implanted and compare the estimated value to the one above which it has been experimentally tested that damages to the devices can be induced ($\sim10^9$ $\frac{n}{cm^2}$) [4].

In the experimental part of the work, CR39 coupled to boron-10 converters were exploited to perform measurements inside a phantom mimicking the human trunk and realistic treatment plans were simulated on it. The results we obtained showed, for the examined cases, that the measured value of the quantity of interest is of the order of $\sim10^5$ $\frac{n}{cm^2 MU}$. Therefore, considering a complete course of radiotherapy in which, in general, a patient receives a dose of about 30 Gy (assuming 100 MU = 1Gy) in fractions of 2 Gy each, the thermal neutron fluence is *below* the one indicated above as certainly critical. Moreover, we performed a study of the neutron fluence distribution inside the phantom which lead to the conclusion that it is approximately constant along the entire axis, but it slightly increases near to the isocenter.

The second part of the work consisted in optimizing and validating the computational model of an Elekta Synergy LINAC head and the bunker where the accelerator is installed at ASUGI, using MCNP. The model of a phantom simulating the presence of a patient in the treatment room was also included. The code was validated by means of experimental thermal neutron fluence measurements at different axial positions inside the phantom. They were performed in two different hospitals where accelerators of the same model as the one simulated are installed. The obtained results look very promising as the simulation describes quite faithfully the radiation transport problem.

Future developments of the present work could be the investigation of the direct damages to cardiac devices when exposed to thermal neutrons fluences of the same order of magnitude we measured. Moreover, RT treatments other

than the one already examined could be analyzed. Lastly, the computational model could be further improved substituting our phantom model with a more realistic anthropomorphic voxel phantom and exploit to simulate real treatment plans.

References

[1] M. Zecchin *et al.*, "Management of patients with cardiac implantable electronic devices (CIED) undergoing radiotherapy: A consensus document from associazione italiana aritmologia e cardiostimolazione (AIAC), Associazione Italiana Radioterapia Oncologica (AIRO), Associazione Italiana Fisica Medica (AIFM)," *International Journal of Cardiology*, vol. 255, pp. 175–183, 3 2018.

[2] M. D. Falco *et al.*, "A randomized in vitro evaluation of transient and permanent cardiac implantable electronic device malfunctions following direct exposure up to 10Gy," *Strahlentherapie und Onkologie*, vol. 197, pp. 198–208, 3 2021.

[3] M. Zecchin *et al.*, "Malfunction of cardiac devices after radiotherapy without direct exposure to ionizing radiation: Mechanisms and experimental data," *Europace*, vol. 18, pp. 288–293, 2 2016.

[4] C. Ferrante, "Study of Neutron-induced Damage to Cardiac Implantable Electronic Devices in Radiation Therapy," Master's thesis, Politecnico di Milano, A.A. 2019-2020.

[5] A. Alem-Bezoubiri *et al.*, "Monte Carlo estimation of photoneutrons spectra and dose equivalent around an 18MV medical linear accelerator," *Radiation Physics and Chemistry*, vol. 97, pp. 381–392, 4 2014.